Clinical Immunology 201 (2019) 35–47

Contents lists available at ScienceDirect

Clinical Immunology

journal homepage: www.elsevier.com/locate/yclim

Hydroxyfasudil alleviates demyelination through the inhibition of MOG antibody and microglia activation in cuprizone mouse model

Jing Wang[a], Ruo-Xuan Sui[b], Qiang Miao[b], Qing Wang[b], Li-Juan Song[b], Jie-Zhong Yu[c], Yan-Hua Li[c], Bao-Guo Xiao[d,*], Cun-Gen Ma[a,b,c,**]

[a] Shanxi Medical University, Taiyuan 030001, China
[b] The Key Research Laboratory of Benefiting Qi for Acting Blood Circulation Method to Treat Multiple Sclerosis of State Administration of Traditional Chinese Medicine, Shanxi University of Traditional Chinese Medicine, Taiyuan 030024, China
[c] Institute of Brain Science, Shanxi Datong University, Datong 037009, China
[d] Institute of Neurology, Huashan Hospital, Institutes of Brain Science and State Key Laboratory of Medical Neurobiology, Fudan University, Shanghai, 200025, China

ARTICLE INFO

Keywords:
Rho kinase
Hydroxyfasudil
Cuprizone-induced demyelination

ABSTRACT

Multiple sclerosis (MS) is an immune-mediated demyelinating disease of the central nervous system characterized by oligodendrocyte loss and progressive neurodegeneration. The cuprizone (CPZ)-induced demyelination is widely used to investigate the demyelination/remyelination. Here, we explored the therapeutic effects of Hydroxyfasudil (HF), an active metabolite of Fasudil, in CPZ model. HF improved behavioral abnormality and reduced myelin damage in the corpus callosum. Splenic atrophy and myelin oligodendrocyte glycoprotein (MOG) antibody were observed in CPZ model, which were partially restored and obviously inhibited by HF, therefore reducing pathogenic binding of MOG antibody to oligodendrocytes. HF inhibited the percentages of $CD4^+IL\text{-}17^+$ T cells from splenocytes and infiltration of $CD4^+$ T cells and $CD68^+$ macrophages in the brain. HF also declined microglia-mediated neuroinflammation, and promoted the production of astrocyte-derived brain derived neurotrophic factor (BDNF) and regeneration of $NG2^+$ oligodendrocyte precursor cells. These results provide potent evidence for the therapeutic effects of HF in CPZ-induced demyelination.

1. Introduction

Multiple sclerosis (MS) is a leading cause of non-traumatic neurological disability, typically characterized by loss of oligodendrocytes and myelin sheaths in white matter of the brain. Despite being with high prevalence in young adults, we are still far from a complete picture in the etiology, pathogenesis and pathophysiology of this disease [1]. There is a growing consensus that the progression of MS is related to myelin destruction (demyelination) [2] and progressive axonal damage [3]. Remyelination is an endogenously regulated process by the generation of new mature oligodendrocytes that provide new myelin sheathes to demyelinated axons, promoting the recovery of axonal integrity and functional deficits [4]. To date, disease-modifying therapies (DMTs) effectively reduce the frequency and severity of MS relapses [5]. However, these immune-modifying drugs are inefficient against primary and secondary non-remitting (progressive) forms of MS [6]. The most current therapies for MS are directed towards modulation of the immune response [7]. However, novel therapies aimed to axonal remyelination are urgently needed.

The cuprizone (CPZ)-induced demyelination, a toxicant-induced demyelination model, is widely used to investigate the demyelination/remyelination that is independent of immune attack [8]. From a pharmaceutical point of view, the CPZ model appeared with selective loss of oligodendrocytes, extensive areas of demyelination and reactive gliosis in the corpus callosum, superior cerebellar peduncles and cerebral cortex [9]. Thus, this model has advantages in studying the regulation of demyelination secondary to toxin-induced oligodendrogliopathy and testing potential therapeutic target for demyelinating diseases.

The Rho kinase (ROCK) is a family of serine-threonine kinase that serves as key downstream effector for Rho GTPases, modulating a wide range of biological processes, including cell contraction and actin organization as well as neurite elongation and neuronal architecture. Because of their broad role in cytoskeletal reorganization, ROCK affects cell migration [10]. ROCK has emerged as major regulators of smooth muscle contraction, stress fiber formation, and focal adhesions by

* Corresponding author.
** Corresponding author at: Shanxi Medical University, Taiyuan 030001, China.
E-mail addresses: bgxiao@shmu.edu.cn (B.-G. Xiao), macungen2001@163.com (C.-G. Ma).

https://doi.org/10.1016/j.clim.2019.01.006
Received 22 July 2018; Received in revised form 14 January 2019; Accepted 14 January 2019
Available online 17 January 2019

regulating actin-myosin contractility [10,11]. MAP2 and neurofilament are neuron-specific substrates for ROCK, and their microtubule polymerizing activity and neurofilament assembly are inhibited by ROCK-mediated phosphorylation [12,13], participating in neurite retraction and neurite outgrowth inhibition [14,15]. Recent studies consider emerging evidence potentially linking ROCK to the pathogenesis of several autoimmune disorders such as Systemic Lupus Erythematosus (SLE), Rheumatoid Arthritis (RA)and MS [16].

Given the potential promise of ROCK as therapeutic targets, Fasudil, a small molecule inhibitor of ROCK, has been proved to have neuroprotective effects in various neurodegenerative diseases, including stroke, experimental autoimmune encephalomyelitis (EAE), Alzheimer's disease (AD), Parkinson's disease (PD) and amyotrophic lateral sclerosis (ALS) [17–21]. Pharmacological ROCK inhibitors protected hippocampal neurons [22] and promoted mobilization of adult neural stem cells [23] after hypoxia/reoxygenation injury, counteracted neurite retraction, stimulated neurite outgrowth in human neuro-2 neurons [24] and promoted axonal regeneration after axonal injury in mice [25,26]. Taken together, ROCK seems to inhibit neurite outgrowth, while ROCK inhibition promotes synapse formation and plasticity, emphasizing its complex and sensitive role on neuronal synapses. In an in vitro model of spinal cord injury (SCI), inhibition of ROCK showed the additive effects on neurite outgrowth and myelination [27]. In EAE, Fasudil regulated T cell responses through inducing the polarization of M2 microglia/macrophages and inhibiting inflammatory responses [22,28,29].

When Fasudil displays certain beneficial effects in treating neurodegenerative/demyelinating disorders, the problem of clinical application obviously limits the use of Fasudil, including short-course treatment, low oral bioavailability, narrower safety window and blood pressure fluctuation. Therefore, we need to develop novel ROCK inhibitors that should have a wider safety window, with low cytotoxicity and blood pressure fluctuation. Hydroxyfasudil (HF), an active metabolite of Fasudil, also inhibits ROCK [30], and has a pharmacological profile similar to that of Fasudil. The area under the plasma concentration–time curve value of HF was approximately 4.5 times higher than that of Fasudil in patients with subarachnoid hemorrhage (SAH) receiving 30 mg of Fasudil [31]. Previous investigations indicate that HF is more selective than Fasudil as an inhibitor of ROCK [32].

The aim of the present study is to observe the potential therapeutic effect of HF for myelin protection and/or regeneration and explore preliminary mechanisms of HF action in a mouse model of CPZ-induced demyelination, providing experimental evidence for further preclinical research.

2. Materials and methods

2.1. Animals

All animal protocols were carried out in strict accordance with the International Council for Laboratory Animal Science guidelines. Ten-week-old male C57BL/6 mice were obtained from Vital River Laboratory Animal Technology Co. Ltd. (Beijing, China). All mice were housed under pathogen-free conditions with a 12-h light/dark cycle and constant temperature (25 ± 2 °C) and relative humidity (55 ± 10%) for one week prior to experimental manipulation. All efforts were made to reduce the number of animals used and their suffering. This study was approved by the Council for Laboratory and Ethics Committee of Shanxi University of Traditional Chinese medicine, Taiyuan, China.

2.2. Induction of demyelination and administration of HF

Mice were exposed to cuprizone (bis(cyclohexanone) oxaldihydrazone; Sigma-Aldrich, USA) in chow (0.2% *w*/w) for a total of 6 weeks. After 4 weeks, mice were randomly divided into three groups: (i) mice received rodent chow as normal group (Normal, $n = 8$); (ii) mice understood demyelination by feeding CPZ diet as CPZ group, with the injection of normal saline (CPZ, n = 8), and (iii) mice understood demyelination, and subsequently treated with HF by intraperitoneal injection (40 mg/kg/day) for consecutive 2 weeks, without CPZ withdrawal (HF, n = 8). HF (from Tianjin Chase Sun Pharmaceutical Co., Ltd., Tian'jin, China.) was dissolved in 0.1% acetic acid, then adjusted pH to 7.0 by sodium carbonate. The CPZ chow was changed every two days and the weight of mice was monitored every other day.

2.3. Behavioral tests

Cuprizone model provokes behavioral changes, affects mood and impairs motor skills [9]. Therefore, we used Elevated plus-maze (EPM) test to measure anxiety on the day before the end of the experiment [33]. Briefly, a mouse was placed in the center area of the plus maze facing an open arm firstly and allowed to move freely through the maze during a 10-min session. The number of entering closed arms was monitored by Limelight video camera based on tracking system.

In addition, the assessment of mice locomotor coordination was performed by Pole test. In brief, mice were placed tenderly head-up facing the apex of the vertical round wood pole with gauze-wrapped rough surface enabling mice to grab (height: 50 cm; diameter: 1 cm). The time of mice descending to the bottom of the pole (touch-down time) was recorded for the evaluation of locomotor coordination. In each test, each mouse conducted three consecutive trials and the average time was recorded for statistical analysis.

2.4. Tissue preparation

Half of the mice in each group were deeply anaesthetized and then perfused intracardially with saline, followed by 4% paraformadehyde (PFA) in phosphate buffer (PBS, 0.01 M, pH 7.4) at the end of experiment. Brains were removed and immediately post-fixed in 4% PFA for 2 h at 4 °C and transferred to 30% *w/v* sucrose solution and kept at 4 °C for approximately 24 h. Coronal frozen sections (10 μm) were sliced on a cryostat microtome (Leica CM1850) and stored at 4 °C for immunofluorescence staining. Another half of the mice were deeply anaesthetized with 10% Chloral hydrate and perfused intracardially with saline. Brains were collected and stored at −80 °C for further analysis.

2.5. Myelin staining and analysis

Luxol Fast Blue (LFB) staining: To examine the extent of demyelination in the corpus callosum, slides of brain were stained with Luxol Fast Blue (LFB). Sections were incubated in LFB solution for 18 h at 60 °C. After washing with distilled water, sections were hydrated with 95% ethanol. Then, the sections were differentiated by 0.05% lithium carbonate solution for 30 s and dipped in 70% alcohol. Finally, sections were dehydrated using graded ethanol and fixed by dimethylbenzene. The areas of demyelination (clear-white) to normal tissue (blue) were quantified.

Black Gold II staining: Black Gold II staining is a widely used method for evaluating demyelination [34]. Brain sections were incubated in pre-warmed Black Gold II solution (AG105, Millipore, Billerica, MA) at 60 °C for 15–25 min until desired signals developed. After rinsing with Milli-Q water for three times, the slides were fixed in the pre-heated 1% sodium thiosulfate (1% in ddH_20) at 60 °C for 3 min. Then the slides were incubated with cresyl violet at room temperature (RT) for 3 min, dehydrated using a series of gradated alcohols and finally cleared in xylene for 2 min. Slides were imaged on Lecia microscope. The demyelination in the corpus callosum was measured using Image Pro Plus software (Media Cybernetics).

MBP immunohistochemistry staining: Brain sections (10 μm) were used for MBP immunohistochemistry staining. The sections were blocked with 1% BSA/PBS for 0.5 h at RT and incubated with anti-myelin basic protein (MBP) (Abcam, USA) overnight at 4 °C, followed

by incubation with corresponding secondary antibody for 2 h at RT. The intensity of MBP staining in the dorsal cerebral cortex and central part of the corpus callosum were imaged on Lecia microscope and analyzed using Image-Pro Plus software in a blinded fashion.

2.6. Preparation of splenic mononuclear cells

At the end of the experiment, mice were sacrificed and spleens were removed under aseptic conditions. The weight and volume of spleen were measured and recorded. Then, suspension of mononuclear cells (MNCs) from spleen was prepared by grinding the tissue through a 40 μm nylon mesh in medium. After erythrocyte lysis and washing, cells were re-suspended (5×10^6/ml) in the complete medium and incubated in the presence or absence of mouse myelin oligodendrocyte glycoprotein peptide$_{35–55}$ (MOG$_{35–55}$, 10 μg/ml, CL. Bio-Scientific. Company, Xi'an, China) for 48 h at 37 °C. The supernatant was collected and stored at −80 °C for ELISA and MOG antibody assay.

2.7. MOG antibody assay

MOG$_{35–55}$ (MEVGWYRSPFSRVVHLYRNGK) and α-synuclein$_{123–140}$ (α-syn$_{123–140}$ (EAYEMPSEEGYQDYEPEA) were produced in an automatic synthesizer (CL. Bio-Scientific Company, Shanghai, China). The purity of the peptide was > 95% as determined by high-performance liquid chromatography.

The serum, supernatant of splenic MNCs and extract of brain homogenate were collected for ELISA and dot blot assay.

ELISA method: Blood was collected from the orbit of mice, then centrifuged at 3000 rpm at 4 °C for 10 min after clotting. Splenic MNCs were incubated in the presence or absence of MOG$_{35–55}$ (10 μg/ml) for 48 h. Brain was homogenized and centrifuged at 12,000 ×*g* for 20 min at 4 °C. MOG$_{35–55}$ (10 μg/ml) dissolved in PBS (pH 7.4) was coated on a 96-well plate (100ul/well) at RT overnight and then blocked with 1% BSA/PBS for 1 h at RT. Diluted samples (serum = 1:100, extract from brain = 1:500) were added and remained at RT for 2 h. After washing with PBST, HRP-conjugated anti-mouse IgG (1:1000, Abcam, USA) was added at RT 1 h, and optical density (OD) value (at 450 nm) was read by multiscan spectrum.

Dot blot method: MOG$_{35–55}$ and α-syn$_{123–140}$ (1 μg/10ul) were coated onto a nitrocellulose membrane (Millipore) overnight at RT. After washing with PBST, the membrane was blocked with 1% BSA/PBS for 1 h at RT. Serum (1:50and 1:200) and culture supernatant were added and remained at RT for 2 h. After washing with PBST, HRP-conjugated anti-mouse IgG (Abcam, USA) was added at RT for 1 h. Immunoblots were developed with an enhanced chemiluminescence system (GE Healthcare Life Sciences) and analyzed using Quantity Software (Bio-Rad, Hercules, CA, USA).

2.8. Cytokine ELISA assay

Interferon-γ (IFN-γ), interleukin 10 (IL-10), IL-17, IL-1β, IL-6, tumour necrosis factor -α (TNF-α) were measured using sandwich ELISA kits (Invitrogen Inc., USA) according to company's instructions. Determination was carried out in triplicate and the concentration of cytokines was expressed as picograms per milliliter.

2.9. Flow cytometry analysis

Splenic MNCs were fixed with 4% PFA for 20 min, and then stained in 0.3% saponin/1% BSA-PBS for 20 min at RT with the following antibodies: FITC-CD4 and PE-IFN-γ/PE-IL-17 (eBioscience), PE-B220 (eBioscience). At least 10, 000 events were collected using flow cytometer (BD Biosciences, USA) and data were analyzed using Cell Quest software.

2.10. Immunofluorescence

After blocking with 1% bovine serum albumin (BSA, Sigma, USA) for 1 h at RT, brain sections were incubated with anti-O4 (1:500, R&D, USA, MAB1326-SP), anti-CD4 (1:200, Abcam, USA, ab25475), anti-CD68 (1:200, Abcam, USA, ab53444), anti-Iba-1 (1:200, Abcam, USA, ab153696), anti-iNOS (1:200, Abcam, USA, ab15323), anti-p-NF-κB/p65 (1:200, Abcam, USA, ab16502), anti-GFAP (1:1000, Abcam, USA, ab4648), anti-BDNF (1:500, Abcam, USA, ab108319) and anti-NG2 (1:1000, Abcam, USA, ab5320) at 4 °C for overnight, followed by corresponding secondary antibodies for 1 h at RT. Results were visualized under fluorescent microscopy, and quantification was analyzed from three sections/mouse by Image-Pro Plus 6.0 software in a blinded fashion.

2.11. Western blot assay

Corpus callosum tissue samples were carefully microdissected using a dissecting microscope and homogenized in RIPA lysis buffer (Beyotime Institute of Biotechnology, PR China). After centrifugation at 12,000 ×*g* for 20 min at 4 °C, the extract was collected and protein concentration was determined by BCA kit (Beyotime Institute of Biotechnology, PR China). Equal amounts of protein (30 μg) were separated on 10% SDS-polyacrylamide gels, and transferred onto a nitrocellulose membrane (Millipore) after electrophoresis. After blocking in 5% non-fat dry milk buffer at RT for 1 h, the membranes were incubated at 4 °C overnight with the following primary antibodies: MBP (1:500, Abcam, USA), BDNF (1:500, Abcam, USA) and β-actin (1:10000, Cell Signaling Technology, USA). Following washes with TBS containing Tween-20, the membranes were incubated with appropriate HRP-conjugated secondary antibody (Earthox LLC, USA) at RT for 2 h. Immunoblots were developed with an enhanced chemiluminescence system (GE Healthcare Life Sciences) and measured using Quantity Software (Bio-Rad, Hercules, CA, USA). The expression of protein was analyzed by normalizing to the expression of the internal control (β-actin).

2.12. Statistical analysis

All the experiments were repeated two or three times. All statistical analyses were performed by one-way analysis of variance (ANOVA) followed by a Bonferroni post hoc test using GraphPad Prism 5 software (Cabit Information Technology Co., Ltd. Shanghai, China). Results are expressed as the mean ± SEM. P value < 0.05 was considered statistically significant.

3. Results

3.1. The improvement of behavioral and pathological changes by HF

As shown in Fig. 1a, the mice fed with CPZ diet lost weight compared to mice with normal diet at the end of first week. In the following 3 weeks, the mice fed with CPZ weighted lower than the normal group and maintained a stable state (Fig. 1a). To further evaluate the induction of demyelination in mice fed with CPZ, the degree of demyelination was determined by Black Gold II staining after 4 weeks of CPZ feeding. The intensity of Black Gold II staining was obviously decreased in the corpus callosum of brain, as compared to normal mice without CPZ feeding (Fig. 1a), demonstrating a demyelinating response to CPZ at the beginning of HF treatment.

To investigate whether HF improve demyelination in CPZ-mediated demyelination, HF or vehicle was administrated after 4 weeks of CPZ feeding for 2 consecutive weeks, while the CPZ diet was maintained up to sixth week (Fig. 1b). Previous studies revealed that CPZ-fed mice exhibited behavioral anxiety and locomotor change [35,36], we first detected the behavioral changes by EMP. Mice fed with CPZ

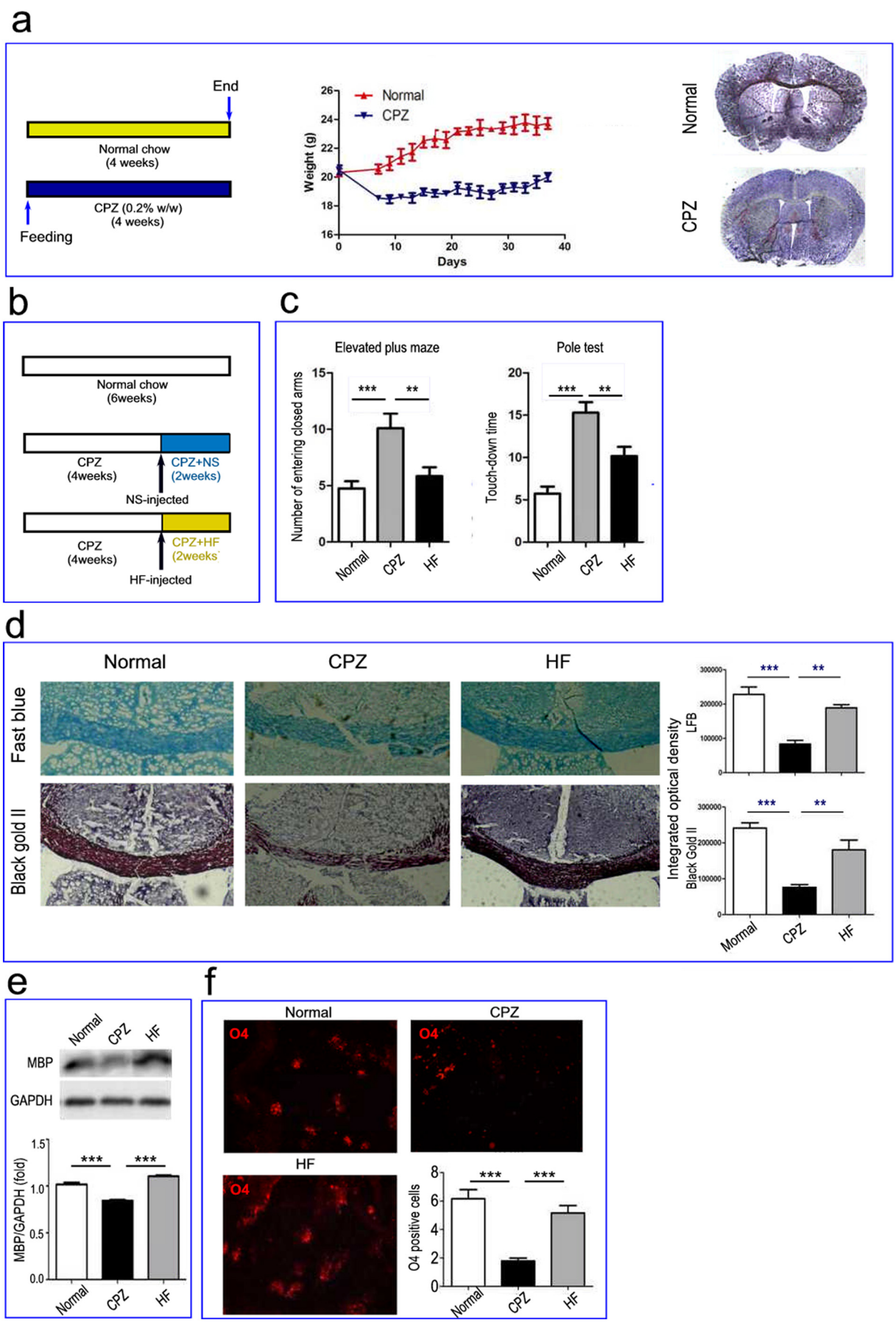

(caption on next page)

Fig. 1. HF improved behavioral abnormality and demyelination. (a) the pattern diagram of CPZ-induced demyelination model before HF treatment, mice were fed with chow containing 0.2% CPZ for 4 weeks. Body weight and Black Gold II staining were recorded and evaluated. (b) the pattern diagram of CPZ-induced demyelination plus HF treatment that was initiated at week 4 after CPZ diet for 2 consecutive weeks, without CPZ withdrawal. The following tests were carried out after 6 weeks of CPZ feeding. (c) EMP and Pole test; (d) Fast blue and Black Gold II staining in the corpus callosum of brain; (e) the expression of MBP protein in the extract of corpus callosum by Western blot; and (f) the numbers of $O4^+$ oligodendrocytes in the striatum by immunohistochemistry. Micrograph are representative of three independent experiments with similar results. All data represents the means ± SEM. **$p < 0.01$, ***$p < 0.001$. (For interpretation of the references to colour in this figure legend, the reader is referred to the web version of this article.)

significantly enhanced the number of entering closed arms (Fig. 1c, $p < 0.001$). In contrast, mice receiving HF administration showed a less entries of closed-arm (Fig. 1c, $p < 0.01$). We also assessed the locomotor coordination using Pole test. Compared to normal group, mice exposed to CPZ recorded a significant extension in touch-down time (Fig. 1c, $p < 0.001$), which was alleviated by HF treatment (Fig. 1c, $p < 0.01$). Overall, HF treatment significantly attenuated the CPZ-induced behavioral anxiety and locomotor change.

To investigate whether the administration of HF improves the demyelination induced by CPZ feeding, we performed LFB and Black-Gold II staining respectively in the corpus callosum. Both LFB and Black gold II staining were significantly weaker in CPZ group (Fig. 1d, $p < 0.001$ respectively). We also detected the expression of MBP in the extract from the corpus callosum of brain by Western blot. The level of MBP protein was significantly decreased following 6 weeks of CPZ feeding, compared to normal group (Fig. 1e, $p < 0.001$). To further assess the main component of myelin sheath, we performed immunofluorescence staining using anti-O4 antibody, a marker for mature oligodendrocytes. As shown in Fig. 1f, CPZ decreased the numbers of $O4^+$ mature oligodendrocytes ($p < 0.001$). These results suggest that exposure to CPZ led to behavioral changes, accompanied by marked demyelination.

HF treatment improved the demyelination, including LFB and Black gold II staining, as compared with CPZ group (Fig. 1d, $p < 0.01$ respectively). In HF group, an increased expression of MBP protein was observed by western blot (Fig. 1e, $p < .001$). The immunofluorescence staining of O4 antibody also indicated that $O4^+$ oligodendrocytes were higher in HF group than that in CPZ group (Fig. 2f, $p < 0.001$). These results clearly demonstrated that the treatment of HF attenuated CPZ-induced demyelination, which is related to the improvement of behavioral changes.

3.2. The partial restoration of spleen atrophy by HF

In mice fed with CPZ, we noted splenic atrophy after 6 weeks of CPZ feeding, as compared to normal mice (Fig. 2a). Atrophic spleens at this time point were about 49% of normal spleen weight (Fig. 2b, $p < 0.001$). Remarkably, the number of splenic MNCs was significantly decreased (Fig. 2c). The treatment of HF partially restored the volume/weight of spleen and number of splenocytes, as compared to CPZ group (Fig. 2a-c. $p < 0.05$).

3.3. The inhibition of MOG specific antibody by HF

It has been proved that the presence of serum autoantibodies to central nervous system-specific proteins was observed in a group of neural or demyelinating injury [37]. Considering that the oligodendrocytes are the main target in CPZ model, we further tested the $MOG_{35–55}$ specific antibody in serum, culture supernatant and brain extract. As shown in Fig. 3a and b, $MOG_{35–55}$ specific antibody was elevated in the serum, culture supernatant and brain extract of mice exposed to CPZ ($p < 0.001$ and $p < 0.05$, respectively). To further evaluate the specificity of the $MOG_{35–55}$ antibody, dot blot assay was carried out by coating $MOG_{35–55}$ and control peptide $\alpha\text{-syn}_{123–140}$ on a nitrocellulose membrane. The results revealed that MOG antibody was positive, while $a\text{-syn}_{123–140}$ antibody was negative (Fig. 3c), suggesting that CPZ feeding resulted in the production of specific $MOG_{35–55}$ antibody. HF treatment effectively decreased the titer of MOG antibody in serum, culture supernatant and brain extract by ELISA and dot blot (Fig. 3a-c, $p < 0.05$, $p < 0.01$ and $p < 0.001$ respectively). These results indicate that the administration of HF reduced the production of MOG antibody in the periphery, which can enter the brain and may cause secondary damage to oligodendrocytes.

Mice exposed to CPZ for 6 weeks indicated slightly higher $B220^+$ B cells in the splenic MNCs than that of the normal controls (Fig. 3d, $p < 0.001$), which was declined by HF administration compared to vehicle controls (Fig. 3d, $p < 0.001$).

To understand whether MOG antibody participates in ongoing cascades of CNS demyelination, we first scanned the myelin structure constructed by MBP immunostaining (Fig. 4a). We next evaluated the binding of MOG-IgG to $O4^+$ oligodendrocytes by adding MOG antibody-positive serum to brain slices of normal mice. It was found that in brain section of normal mice, the overlapping of O4 and IgG immunostaining was seen in both striatum and ventral pallidum of brain (Fig. 4b), suggesting that there was a specific binding of MOG antibody to $O4^+$ oligodendrocytes. We further compared the binding of MOG-IgG to $O4^+$ oligodendrocytes in the sections of brain from normal, CPZ and CPZ + HF mice. The results showed that compared to normal mice, the density of IgG staining in brain section of CPZ and CPZ + HF mice was increased on $O4^+$ oligodendrocyte, accompanied by the damage of oligodendrocytes, especially in CPZ mice (Fig. 4c), therefore revealing that MOG antibody that penetrates into the brain can bind to oligodendrocytes and cause the damage of oligodendrocytes.

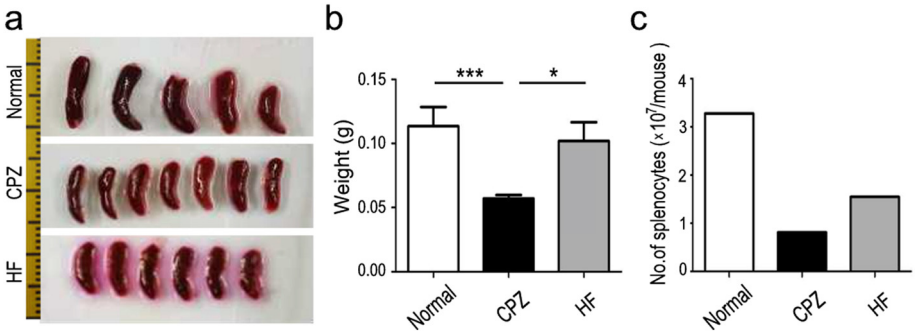

Fig. 2. HF partially restored spleen atrophy. (a) the photograph of spleen volume; (b) the weight of spleens, and (c) the numbers of splenic MNCs in each group. All data represents the means ± SEM. *$p < 0.05$, ***$p < 0.001$.

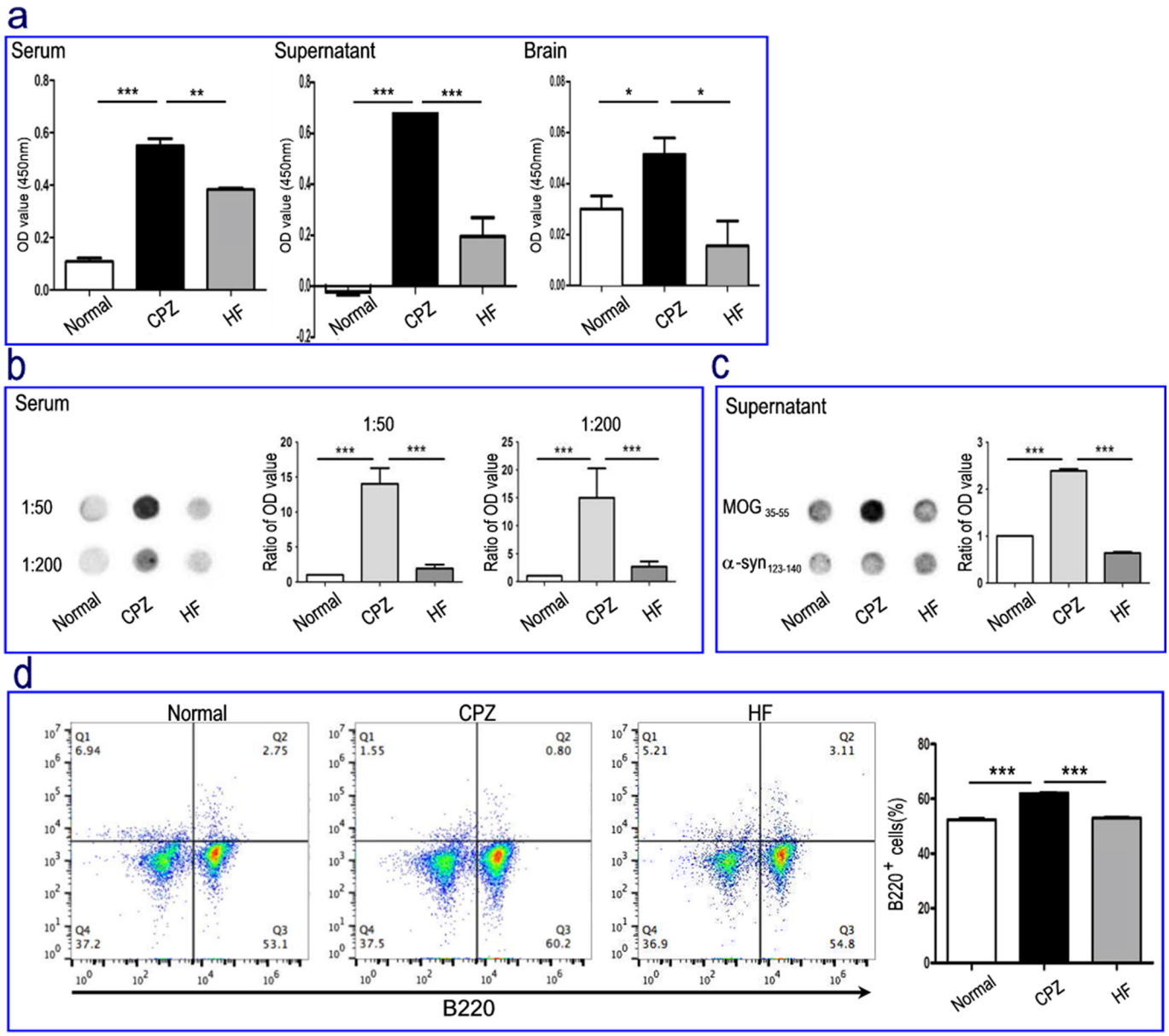

Fig. 3. HF inhibited the production of specific MOG antibody. (a) the titer of MOG antibody in serum (1:100), supernatant of splenocytes and extract of brains (1:500) was measured by ELISA. (b) the titer of MOG antibody in serum (1:50 and 1:200) was measured by dot blot. (c) the specificity of MOG antibody in serum was defined for coating $MOG3_{5–55}$ and $\alpha\text{-syn}_{123–140}$ by dot blot. (d) the percentage of $B220^+$ B cells in splenocytes was measured by flow cytometry. All data represents the means ± SEM. *$p < 0.05$, **$p < 0.01$, ***$p < 0.001$.

3.4. The alternation of T cell responses by HF

Next, taking account of these changes in spleen volume and MOG antibody induced by CPZ exposure, we further evaluated whether these unexpected results may be related to T cell responses. As compared to normal group, CPZ exposure reduced $CD4^+IFN\text{-}\gamma^+$ T cells (Fig. 5a, $p < 0.01$), while HF treatment significantly inhibited $CD4^+IL\text{-}17^+$ T cells (Fig. 5a, $p < 0.01$) and slightly enhanced $CD4^+IFN\text{-}\gamma^+$ T cells (no statistical difference). The results from brain immunohistochemistry showed that a few of infiltrated $CD4^+$ T cells and $CD68^+$ macrophages were detected in mice fed with CPZ (Fig. 5b, $p < 0.001$ respectively), which was inhibited by HF administration (Fig. 5b, $p < 0.001$ respectively).

3.5. The alternation of the neuroinflammation and neurotrophic factor by HF

The CPZ model of demyelination is characterized by loss of mature oligodendrocytes, accompanied by neuroinflammation. Microglia are activated after neuronal injury and demyelination and are the major source of neuroinflammation in the CNS, further amplifying secondary damage to neurons and myelin sheaths. The CPZ exposure increased the number of $Iba1^+$ microglia in the striatum of brain, which are inhibited by HF administration (Fig. 6a).

iNOS is an important marker of inflammatory M1 microglia, while NF-κB is a key modulator in promoting an inflammatory response of microglia. The CPZ exposure induced $Iba1^+iNOS^+$ and $Iba1^+p\text{-NF-κB/p65}^+$ microglia in the striatum of brain compared to normal mice (Fig.6b and c, $p < 0.001$ respectively). The administration of HF effectively declined the numbers of $Iba1^+iNOS^+$ and $Iba1^+p\text{-NF-κB/p65}^+$ microglia, as compared to CPZ mice (Fig. 6b and c, $p < 0.001$

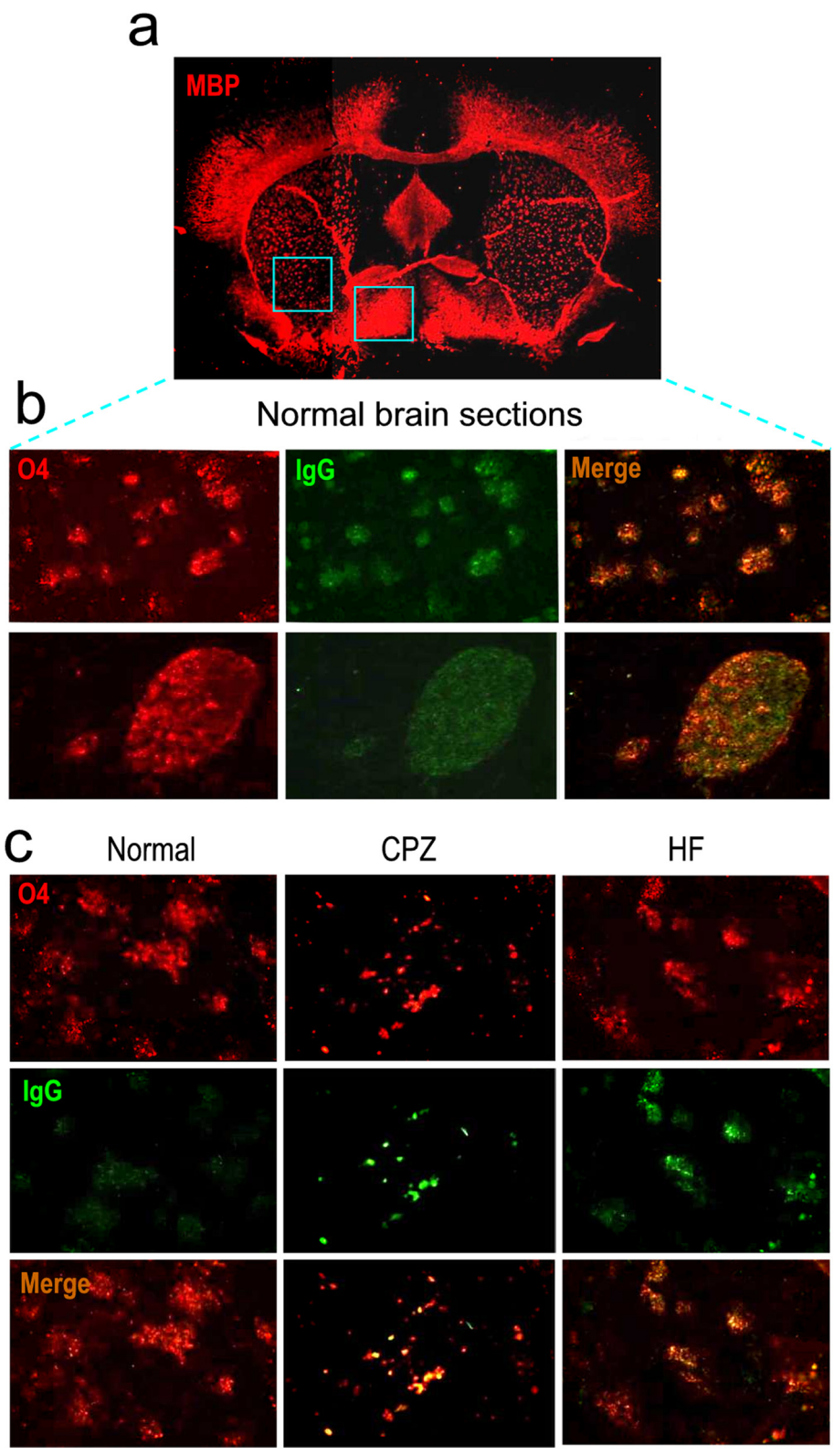

Fig. 4. MOG antibody bound to $O4^+$ oligodendrocytes, which may be related with the damage of oligodendrocytes. (a) computer mapping of MBP immunohistochemistry staining in mouse brain (blue square on the left = the striatum and blue square on the right = ventral pallidum). (b) in normal brain section, the binding of MOG antibody IgG to $O4^+$ oligodendrocytes in the striatum and ventral pallidum was detected by using MOG antibody positive serum from CPZ-fed mice. (c) in brain section from normal, CPZ and CPZ + HF mice, the binding of MOG antibody IgG to $O4^+$ oligodendrocyte was detected in the striatum. Micrograph are representative of three independent experiments with similar results. (For interpretation of the references to colour in this figure legend, the reader is referred to the web version of this article.)

respectively).

As expected, the CPZ exposure elevated the production of inflammatory cytokine IL-1β, IL-6 and TNF-α in the brain compared to normal mice (Fig. 6d, $p < 0.001$ respectively), although the increase of TNF-α did not reached statistical difference. The administration of HF inhibited the increase of IL-1β and IL-6 (Fig. 6d, $p < 0.001$ respectively). These results indicated that CPZ exposure triggered neuroinflammation that may be caused by inflammatory M1 microglia, while HF attenuated inflammatory microenvironment by inhibiting inflammatory M1 microglia in the brain.

It is generally accepted that astrocytes support oligodendrocyte function. Astrocyte-derived BDNF supports myelin protein synthesis after CPZ-induced demyelination [38]. The results showed that CPZ exposure caused the enrichment of $GFAP^+$ astrocytes in the corpus

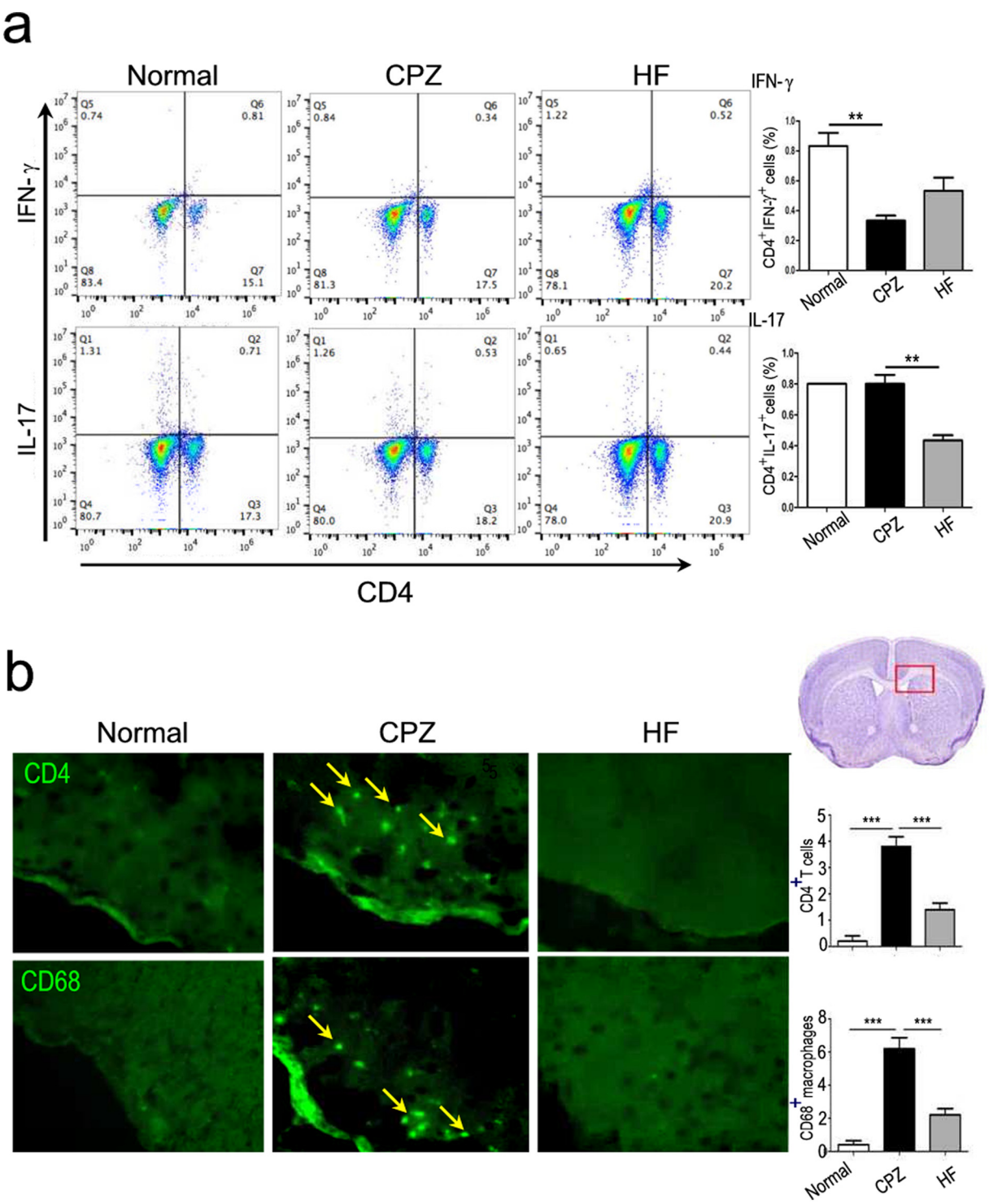

Fig. 5. HF influenced T cell subgroup and inflammatory infiltration in the brain. (a) splenic MNCs were stained and analyzed by low cytometry. (b) the infiltration of $CD4^+$ T cells and $CD68^+$ macrophages in the brain section (red box in the brain pattern = region of photos) was measured by immunohistochemistry staining. Micrograph are representative of three independent experiments with similar results. All data represents the means ± SEM. $^{**}p < 0.01$, $^{***}p < 0.001$. (For interpretation of the references to colour in this figure legend, the reader is referred to the web version of this article.)

callosum of brain (Fig. 7a). However, the administration of HF did not change the enrichment of $GFAP^+$ astrocytes compared to CPZ group (Fig. 7a). In the striatum, the CPZ exposure also obviously induced the increase of $GFAP^+$ astrocytes, while the administration of HF further increased the numbers of $GFAP^+$ astrocytes (Fig. 7a). Most importantly, the administration of NF induced an increased BDNF immunoreactivity that was entirely co-localized with $GFAP^+$ astrocytes (Fig. 7b). Meanwhile, the expression of BDNF protein in the brain was increased in CPZ-fed mice (Fig. 7c, $p < 0.05$) and further elevated dramaticly in HF-treated mice as compared to CPZ-fed mice (Fig. 7c, $p < 0.05$).

BDNF deficiency restricts the proliferation of oligodendrocyte progenitors following CPZ-induced demyelination [39]. As shown in Fig. 7d, the administration of HF induced the generation of $NG2^+$ oligodendrocyte progenitors in the corpus callosum, which may be related

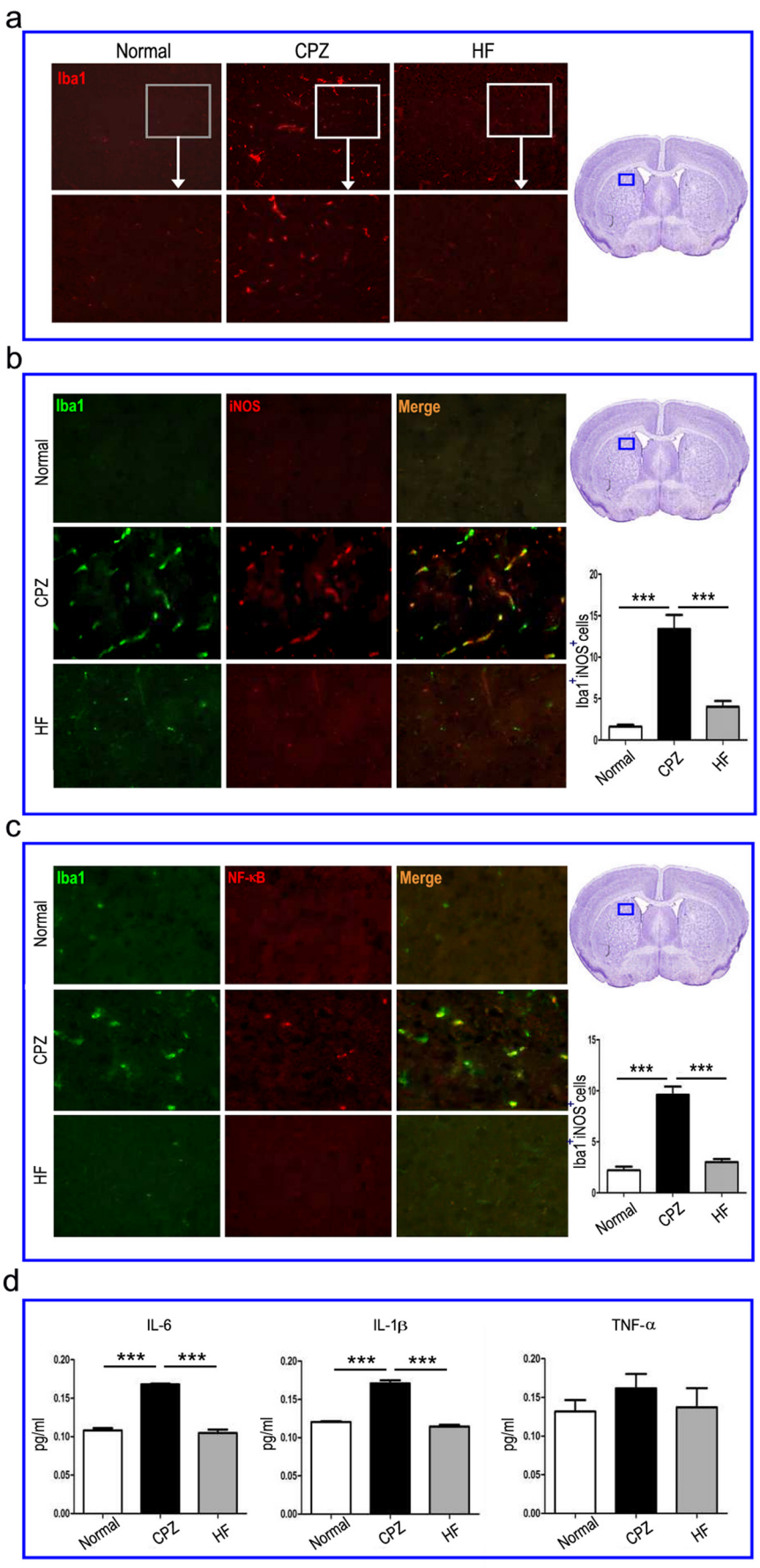

Fig. 6. HF inhibited microglia-mediated inflammatory microenvironment in the brain. (a) microglia were stained with anti-Iba1 antibody, and $Iba1^+$ microglia were observed in the striatum near the corpus callosum, with different magnification. (b) the number of $Iba1^+$ microglia expressing iNOS was counted in the striatum near the corpus callosum. (c) the number of $Iba1^+$ microglia expressing p-NF-κB/p65 was counted in the striatum near the corpus callosum. (d) the concentration of IL-6, IL-1β and TNF-α in extract of brain was measured by ELISA. Micrograph are representative of three independent experiments with similar results. All data represents the means ± SEM. ***$p < 0.001$.

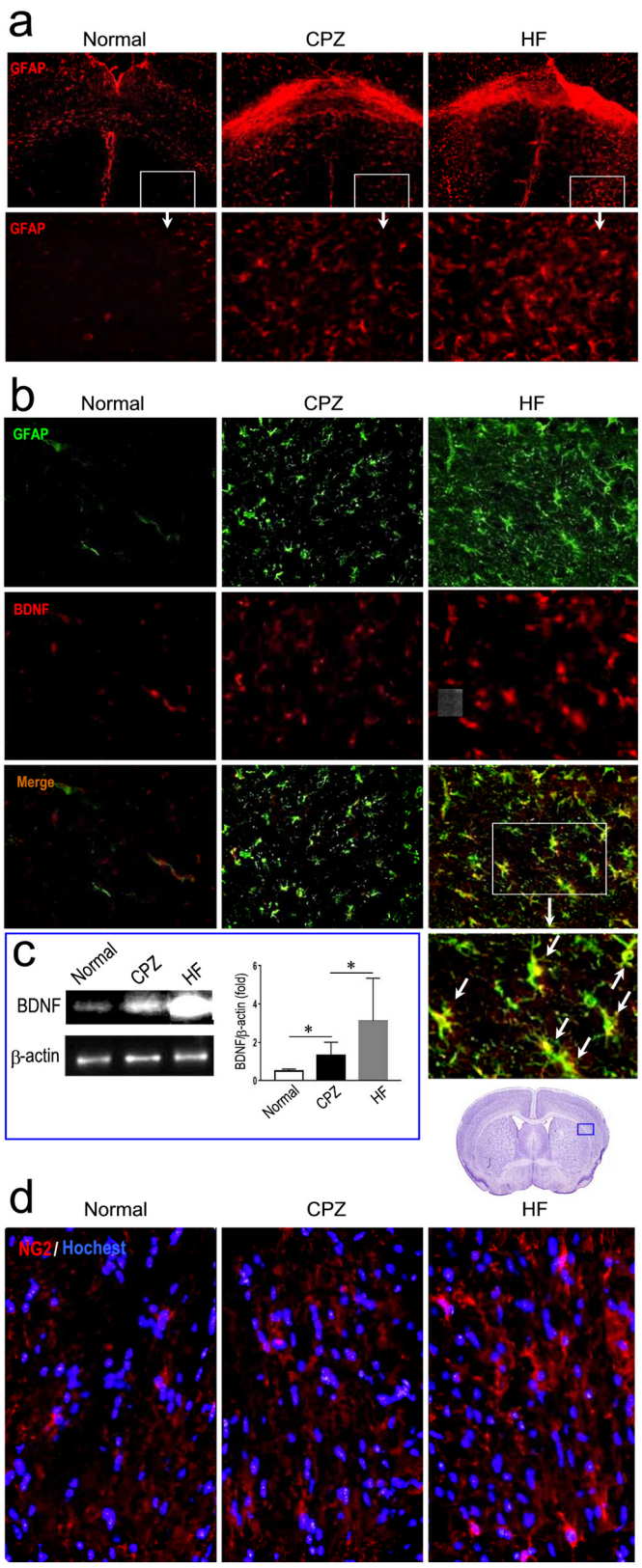

Fig. 7. HF induced astrocyte-derived BDNF and NG2$^+$ oligodendrocyte progenitors in the brain. (a) astrocytes were stained with anti-GFAP antibody, and the enrichment of GFAP$^+$ astrocytes in the corpus callosum was observed. (b) GFAP$^+$ astrocytes expressing BDNF in the striatum near the corpus callosum were observed. (c) the expression of BDNF protein in the brain was measured by western blot. (d) NG2$^+$ oligodendrocyte progenitors were stained with NG2 antibody (blue box in the brain pattern = region of photos). Micrograph are representative of three independent experiments with similar results. All data represents the means ± SEM. *$p < 0.05$. (For interpretation of the references to colour in this figure legend, the reader is referred to the web version of this article.)

to increased production of astrocyte-derived BDNF.

4. Discussion

In the present study, mice showed obvious demyelinating lesions after 4 weeks of CPZ feeding, which was significantly improved by subsequent HF treatment. Simultaneously, HF decreased the damage of O4$^+$ oligodendrocytes, accompanied by the inhibition of microglia-mediated neuroinflammation and the induction of astrocyte-derived BDNF and NG2 oligodendrocyte progenitors in the brain. White matter damage has been linked to emotional and behavioral deficits [40]. Previous studies in demyelinating MS have demonstrated that white matter abnormalities have received increasing interest related to psychiatric disorders. Mice exposed to CPZ showed a series of abnormal behaviors mimicking the complex symptoms observed in psychiatric disorders [41]. Besides, abnormal behaviors of CPZ-fed mice were not absolutely contributed by the white matter damage, according to the previous report that increased concentrations of inflammatory cytokines could play an essential role in this abnormal behavior. For example, central blockade of IL-1β reversed the anxiety-like phenotype, revealing that neuroinflammation contributes to the complex neurobiological mechanisms underlying mood disorders [42].

Here, we observed two discoveries for the first time in CPZ-induced demyelination model. One is the appearance of splenic atrophy, and the other one is the production of anti-$MOG_{35–55}$ antibody. A study from another laboratory displayed that patients undergoing acute ischemic stroke (< 24 h) showed marked splenic atrophy measured by magnetic resonance imaging [43]. Moreover, the decrease of spleen volume had been found in transient MCAO model of mice [44,45], which may be related to apoptosis of cells and loss of functional centers within spleen [44]. Another study showed that the weight of spleen in acute EAE was also decreased, but no remarkable changes were observed microscopically except slight reduction of the white pulp [46]. As a result, this phenomenon has not attracted further attention. At present, we still lack direct evidence to explain the causes and significance of splenic atrophy. It was reported that activated α1-adrenergic receptors were found on splenic capsule after catecholamine surge following MCAO [47]. The splenic atrophy was prevented by blocking the α1-adrenergic receptors with prazosin or carvedilol at 48 h following MCAO [48]. In addition, the stress response in the hippocampus appear to play an intricate role in altered spleen size [49]. Of course, this can't be completely ruled out that CPZ feeding may directly mediate splenic atrophy, because polycyclic aromatic hydrocarbon can induce splenic atrophy [50]. Although the mechanism of splenic atrophy in CPZ demyelination is still not clear, HF treatment can partially restore the size of spleen and the number of splenocytes.

Next, how do we understand that CPZ feeding produced MOG antibody? Some studies found that the destruction of neural cells or oligodendrocytes lead to release of damage-associated molecular patterns (DAMPs) to the extra cellular environment, initiating immune response [51]. MOG produced by myelin destruction also induced a strong B-cell response, probably because of its accessibility to antibodies on the outer lamellae of myelin and on the plasma membrane of myelinating oligodendrocytes [52,53]. Another study demonstrated that debris from damaged cells in the nervous system may present as antigens, giving rise to autoantibodies. Therefore, it is possible that the DAMPs or myelin debris are released into the blood circulation by BBB and/or CNS-draining lymph nodes, and potentially activate the innate immune system. In line with these observations, our results demonstrated that

MOG antibody was detected in serum and supernatant of cultured splenocytes.

Our results showed that: 1) the titer of MOG antibody in the brain of CPZ-treated mice was higher than that of normal mice, suggesting that MOG antibody produced by peripheral immune cells can penetrate into the brain; 2) anti α-syn antibody was negative, incidentally revealing that dopamine neurons may be not involved in this study, except demyelination. Here, we are trying to explain whether MOG antibody can further cause oligodendrocyte damage in the CNS. In vivo models showed that B cells and SCI-induced antibodies exacerbate tissue damage and impair neurological recovery after SCI [54]. Antibodies to GalC and MOG can play a major role in destabilizing myelin through MBP breakdown [55]. To date, the pathogenic function of CNS-specific antibodies is generally projected into enhancing ongoing inflammatory demyelination [54]. In the current study, human MS patients have circulating antibodies specific for both human and mouse MOG. MOG-specific antibodies from MS patients exacerbated disease in a humanized mouse model, providing definitive evidence for the contribution of MOG-specific antibodies to MS [56]. Our results showed that MOG antibody was elevated in the brain of mice fed with CPZ, and can bind to $O4^+$ oligodendrocytes, providing a possibility for specific MOG antibody-mediated oligodendrocyte damage. Therefore, it is logical to explore the inhibition of B cell function as a therapeutic option.

The next question is by which HF inhibited the production of $MOG_{35–55}$ specific antibody. We hypothesized HF inhibited MOG antibody possibly by direct or indirect two routes: 1) the protection of myelin sheath can decrease DAMPs and myelin debris, thereby reducing the production of MOG antibody stimulated by DAMPs and myelin debris in blood circulation, and 2) the protection of myelin sheath also decreases microglia-mediated inflammatory response, thereby preventing the damage to endothelial cells and the entry of DAMPs and myelin debris into blood circulation. However, we can't exclude the direct action of HF on B cells, inhibiting the production of MOG antibody. Recent study found that Fasudil, a ROCK inhibitor, impaired the antibody response through decreasing $CD19^+$ B cells, especially germinal center B cells in experimental autoimmune myestenia gravis (EAMG) rats [57]. The results from our Lab also found that Fasudil reduced the production of autoantibodies by directly inhibiting the differentiation of plasma cells (unpublished data). The weight of MOG antibody in the demyelination still needs further exploration and confirmation.

In addition to demyelination caused by MOG antibody, microglia exert inflammatory neurotoxic function in the CPZ model [58]. Myelin is also a potent microglia stimulus, resulting in microglia-mediated neuroinflammation. Thus, CPZ-induced demyelination is characterized by microglia response [59] that produce inflammatory cytokines, which have been implicated in the process of demyelination. In a recent study, the death of oligodendrocytes in vivo is enforced by local glial activation [60]. However, activated microglia also play important roles in protection against various pathological conditions in the CNS [61]. In this study, the CPZ exposure induced $Iba1^+$ microglia expressing iNOS and p-NF-κB/p65, accompanied by the increase of inflammatory cytokine IL-1β, IL-6 and TNF-α in the brain. Since oligodendrocytes are highly vulnerable under the inflammatory microenvironment, HF enhanced oligodendrocyte survival and improved neurological deficits possibly through reducing microglia-mediated neuroinflammation in the demyelination/remyelination process.

Previous studies demonstrated that BDNF enhances DNA synthesis and differentiation of oligodendrocytes through the trkB receptor [62]. Mice with reduced BDNF ($BDNF^{+/-}$ mice) lead to the deficits of $NG2^+$ progenitors and myelin proteins [63], suggesting that BDNF is important for the development of oligodendrocytes in vivo. Astrocyte-derived BDNF supports myelin protein synthesis after CPZ-induced demyelination [63]. Our results showed that HF treatment increased the numbers of $GFAP^+$ astrocytes in the striatum, in which astrocytes expressing BDNF were obviously enhanced, suggesting that astrocyte-derived BDNF should contribute to the protection and/or regeneration of myelin sheath. Clinical data from MS patients also implicates BDNF as a therapeutic target in the demyelinating diseases. BDNF increased in MS patients after recovery from the relapsing phase of relapsing-remitting MS (RRMS), suggesting that BDNF may contribute to the recovery [64–66]. Further, MNCs from MS patients treated with Glatiramer acetate (GA) and IFN-β exhibited higher levels of BDNF than that from patients treated with other drugs [67,68], therefore revealing that current MS therapies may be to increase BDNF in MS patients, leading to protective effects. Consistent with these observations, HF treatment induced the expression of astrocyte-derived BDNF, accompanied by the regeneration of $NG2^+$ oligodendrocyte progenitors.

In conclusion, our results demonstrated that HF treatment improved behavioral change, relieved CPZ-induced demyelination and alleviated inflammatory microenvironment, possibly by inhibiting MOG antibody and microglia/infiltrating cell-mediated neuroinflammation and inducing astrocyte-derived BDNF and $NG2^+$ oligodendrocyte progenitors in the brain. These data provide potential therapeutic strategy to alleviate demyelination or induce remyelination in the treatment of MS or other related diseases. However, the accurate mechanisms of HF action and the correlation between these manifestations remain to be further studied.

Supplementary data to this article can be found online at https://doi.org/10.1016/j.clim.2019.01.006.

Funding

This work was supported by project grants from the National Natural Science Foundation of China (81473577), Research Project Supported by Shanxi Scholarship Council of China (2014-7), and the 2011 Cultivation Project of Shanxi University of Chinese Medicine (No. 2011PY-1), Health and Family Planning Commission of Shanxi Province (201601112).

Conflict of interest

The authors declare no financial or commercial conflict of interest.

Acknowledgement

Ruo-Xuan Sui: data statistics, Qiang Miao: experimental operation, Qing Wang: writing assistance, Li-Juan Song: proof reading the article, Jie-Zhong Yu: writing assistance, Yan-Hua Li: proof reading the article, Bao-Guo Xiao: designing the experiment; providing language help, Cun-Gen Ma: designing the experiment; providing language help.

References

[1] C. Stadelmann, Multiple sclerosis as a neurodegenerative disease: pathology, mechanisms and therapeutic implications, Curr. Opin. Neurol. 24 (2011) 224–229.
[2] R.J. Franklin, Why does remyelination fail in multiple sclerosis? Nat. Rev. Neurosci. 3 (2002) 705–714.
[3] B.D. Trapp, R.M. Peterson, R. Ransohoff, S. Rudick, L. Mork, L. Bo, Axonal transection in the lesions of multiple sclerosis, N. Engl. J. Med. 338 (1998) 278–285.
[4] R.J. Franklin, C. Ffrench-Constant, Remyelination in the CNS: from biology to therapy, Nat. Rev. Neurosci. 9 (2008) 839–855.
[5] A. Rae-Grant, G.S. Day, R.A. Marrie, A. Rabinstein, B.A.C. Cree, G.S. Gronseth, M. Haboubi, J. Halper, J.P. Hosey, D.E. Jones, R. Lisak, D. Pelletier, S. Potrebic, C. Sitcov, R. Sommers, J. Stachowiak, T.S.D. Getchius, S.A. Merillat, T. Pringsheim, Comprehensive systematic review summary: Disease-modifying therapies for adults with multiple sclerosis, Neurology 90 (2018) 789–800.
[6] R.N. Narayan, T. Forsthuber, O. Stüve, Emerging drugs for primary progressive multiple sclerosis, Expert Opin. Emerg. Drugs 23 (2018) 97–110.
[7] H.F. McFarland, R. Martin, Multiple sclerosis: a complicated picture of autoimmunity, Nat. Immunol. 8 (2007) 913–919.
[8] W.F. Blakemore, R.J.M. Franklin, Remyelination in experimental models of toxin-induced demyelination, Curr. Top. Microbiol. Immunol. 318 (2008) 193–212.
[9] J.M. Vega-Riquer, G. Mendez-Victoriano, R.A. Morales-Luckie, O. Gonzalez-Perez, Five decades of cuprizone, an updated model to replicate demyelinating diseases, Curr. Neuropharmacol. (2017), https://doi.org/10.2174/1570159x15666170717120343.

[10] M. Amano, M. Nakayama, K. Kaibuchi, Rho-kinase/ROCK: a key regulator of the cytoskeleton and cell polarity, Cytoskeleton 67 (2010) 545–554.
[11] A.V. Schofield, O. Bernard, Rho-associated coiled-coil kinase (ROCK) signaling and disease, Crit. Rev. Biochem. Mol. Biol. 48 (2013) 301–316.
[12] R. Hashimoto, Y. Nakamura, H. Goto, Y. Wada, S. Sakoda, K. Kaibuchi, M. Inagaki, M. Takeda, Domain- and site-specific phosphorylation of bovine NF-L by Rho-associated kinase, Biochem. Biophys. Res. Commun. 245 (1998) 407–411.
[13] M. Amano, T. Kaneko, A. Maeda, M. Nakayama, M. Ito, T. Yamauchi, H. Goto, Y. Fukata, N. Oshiro, A. Shinohara, A. Iwamatsu, K. Kaibuchi, Identification of Tau and MAP2 as novel substrates of Rho-kinase and myosin phosphatase, J. Neurochem. 87 (2003) 780–790.
[14] M. Amano, K. Chihara, N. Nakamura, Y. Fukata, T. Yano, M. Shibata, M. Ikebe, K. Kaibuchi, Myosin II activation promotes neurite retraction during the action of Rho and Rho-kinase, Genes Cells 3 (1998) 177–188.
[15] M. Hirose, T. Ishizaki, N. Watanabe, M. Uehata, O. Kranenburg, W.H. Moolenaar, F. Matsumura, M. Maekawa, H. Bito, S. Narumiya, Molecular dissection of Rho-associated protein kinase-regulated neurite remodeling in neuroblastoma N1E-115 cells, J. Cell Biol. 141 (1998) 1625–1636.
[16] A.B. Pernis, E. Ricker, C.H. Weng, C. Rozo, W. Yi, Rho kinases in autoimmune diseases, Annu. Rev. Med. 67 (2016) 355–374.
[17] T. Fukuta, T. Asai, A. Sato, M. Namba, Y. Yanagida, T. Kikuchi, H. Koide, K. Shimizu, N. Oku, Neuroprotection against cerebral ischemia/reperfusion injury by intravenous administration of liposomal fasudil, Int. J. Pharm. 506 (2016) 129–137.
[18] S.W. Hou, C.Y. Liu, Y.H. Li, J.Z. Yu, L. Feng, Y.T. Liu, M.F. Guo, Y. Xie, J. Meng, H.F. Zhang, B.G. Xiao, C.G. Ma, Fasudil ameliorates disease progression in experimental autoimmune encephalomyelitis, acting possibly through antiinflammatory effect, CNS. Neurosci. Ther. 18 (2012) 909–917.
[19] J.Z. Yu, Y.H. Li, C.Y. Liu, Q. Wang, Q.F. Gu, H.Q. Wang, G.X. Zhang, B.G. Xiao, C.G. Ma, Multitarget therapeutic effect of Fasudil in APP/PS1transgenic mice, CNS. Neurol. Disord. Drug Targets 16 (2017) 199–209.
[20] L. Tonges, T. Frank, L. Tatenhorst, K.A. Saal, J.C. Koch, E.M. Szego, M. Bahr, J.H. Weishaupt, P. Lingor, Inhibition of rho kinase enhances survival of dopaminergic neurons and attenuates axonal loss in a mouse model of Parkinson's disease, Brain 135 (2012) 3355–3370.
[21] L. Tonges, R. Gunther, M. Suhr, J. Jansen, A. Balck, K.A. Saal, E. Barski, T. Nientied, A.A. Gotz, J.C. Koch, B.K. Mueller, J.H. Weishaupt, M.W. Sereda, U.K. Hanisch, M. Bahr, P. Lingor, Rho kinase inhibition modulates microglia activation and improves survival in a model of amyotrophic lateral sclerosis, Glia 62 (2014) 217–232.
[22] J. Ding, Q.Y. Li, X. Wang, C.H. Sun, C.Z. Lu, B.G. Xiao, Fasudil protects hippocampal neurons against hypoxia-reoxygenation injury by suppressing microglial inflammatory responses in mice, J. Neurochem. 114 (2010) 1619–1629.
[23] J. Ding, Q.Y. Li, J.Z. Yu, X. Wang, C.H. Sun, C.Z. Lu, B.G. Xiao, Fasudil, a Rho kinase inhibitor, drives mobilization of adult neural stem cells after hypoxia/reoxygenation injury in mice, Mol. Cell. Neurosci. 43 (2010) 201–208.
[24] P. Lingor, N. Teusch, K. Schwarz, R. Mueller, H. Mack, M. Bahr, B.K. Mueller, Inhibition of Rho kinase (ROCK) increases neurite outgrowth on chondroitin sulphate proteoglycan in vitro and axonal regeneration in the adult optic nerve in vivo, J. Neurochem. 103 (2007) 181–189.
[25] A. Hiraga, S. Kuwabara, H. Doya, K. Kanai, M. Fujitani, J. Taniguchi, K. Arai, M. Mori, T. Hattori, T. Yamashita, Rho-kinase inhibition enhances axonal regeneration after peripheral nerve injury, J. Peripher. Nerv. Syst. 11 (2006) 217–224.
[26] C. Chen, J.Z. Yu, Q. Zhang, Y.F. Zhao, C.Y. Liu, Y.H. Li, W.F. Yang, C.G. Ma, B.G. Xiao, Role of Rho kinase and Fasudil on synaptic plasticity in multiple sclerosis, NeuroMolecular Med. 17 (2015) 454–465.
[27] S.D. Boomkamp, M.O. Riehle, J. Wood, M.F. Olson, S.C. Barnett, The development of a rat in vitro model of spinal cord injury demonstrating the additive effects of Rho and ROCK inhibitors on neurite outgrowth and myelination, Glia 60 (2012) 441–456.
[28] C.G. Ma, C.Y. Liu, J.Z. Yu, Y.H. Li, H.F. Zhang, M.F. Guo, L. Feng, J.J. Huang, B.G. Xiao, BG, Polarization of macrophages and T cells to anti-inflammation in EAE mice treated with Fasudil, J. Neurol. Sci. 333 (2013) e419.
[29] C. Chen, Y.H. Li, Q. Zhang, J.Z. Yu, Y.F. Zhao, C.G. Ma, B.G. Xiao, Fasudil regulates T cell responses through polarization of BV-2 cells in mice experimental autoimmune encephalomyelitis, Acta Pharmacol. Sin. 35 (2014) 1428–1438.
[30] M. Shibuya, S. Hirai, M. Seto, S.I. Satoh, E. Ohtomo, Fasudil Ischemic Stroke Study Group: Effects of fasudil in acute ischemic stroke: results of a prospective placebo-controlled double-blind trial, J. Neurol. Sci. 238 (2005) 31–39.
[31] Y. Suzuki, M. Shibuya, S. Satoh, H. Sugiyama, M. Seto, K. Takakura, Safety and efficacy of fasudil monotherapy and fasudil-ozagrel combination therapy in patients with subarachnoid hemorrhage: sub-analysis of the post-marketing surveillance study, Neurol. Med. Chir. 48 (2008) 241–247.
[32] S. Satoh, M. Takayasu, K. Kawasaki, I. Ikegaki, A. Hitomi, K. Yano, M. Shibuya, T. Asano, Antivasospastic effects of hydroxyfasudil, a Rho-kinase inhibitor, after subarachnoid hemorrhage, J. Pharmacol. Sci. 118 (2012) 92–98.
[33] A.P. Carobrez, L.J. Bertoglio, Ethological and temporal analyses of anxiety-like behavior: the elevated plus-maze model 20 years on, Neurosci. Biobehav. Rev. 29 (2005) 1193–1205.
[34] K. Yoshikawa, S. Palumbo, C.D. Toscano, F. Bosetti, Inhibition of 5-lipoxygenase activity in mice during cuprizone-induced demyelination attenuates neuroinflammation, motor dysfunction and axonal damage, Prostaglandins Leukot. Essent. Fatty Acids 85 (2011) 43–52.
[35] H. Xu, H.J. Yang, Y. Zhang, R. Clough, R. Browning, X.M. Li, Behavioral and neurobiological changes in C57BL/6 mice exposed to cuprizone, Behav. Neurosci. 123 (2009) 418–429.
[36] H. Zhang, Y. Zhang, H. Xu, L. Wang, J. Zhao, J. Wang, Z. Zhang, Q. Tan, J. Kong, Q. Huang, X.M. Li, Locomotor activity and anxiety status, but not spatial working memory, are affected in mice after brief exposure to cuprizone, Neurosci. Bull. 29 (2013) 633–641.
[37] D.P. Ankeny, P.G. Popovich, PG, B cells and autoantibodies: complex roles in CNS injury, Trends Immunol. 31 (2010) 332–338.
[38] M.W. VonDran, H. Singh, J.Z. Honeywell, C.F. Dreyfus, Levels of BDNF impact oligodendrocyte lineage cells following a cuprizone lesion, J. Neurosci. 31 (2011) 14182–14190.
[39] V. Tsiperson, Y. Huang, I. Bagayogo, Y. Song, M.W. VonDran, E. DiCicco-Bloom, C.F. Dreyfus, Brain-derived neurotrophic factor deficiency restricts proliferation of oligodendrocyte progenitors following cuprizone-induced demyelination, ASN. Neuro. 7 (2015) (pii: 1759091414566878).
[40] J. Chun, H.P. Hartung, HP, Mechanism of action of oral fingolimod (FTY720) in multiple sclerosis, Clin. Neuropharmacol. 33 (2010) 91–101.
[41] Y. Xiu, G.H. Cheng, C. Peng, Y. Wang, Y.D. Li, F.L. Chao, Y. Tang, Ultrastructural abnormalities and loss of myelinated fibers in the corpus callosum of demyelinated mice induced by cuprizone, J. Neurosci. Res. 95 (2017) 1677–1689.
[42] A. Gentile, D. Fresegna, A. Musella, H. Sepman, S. Bullitta, F. De Vito, R. Fantozzi, A. Usiello, M. Maccarrone, N.B. Mercuri, B. Lutz, G. Mandolesi, D. Centonze, Interaction between interleukin-1β and type-1 cannabinoid receptor is involved in anxiety-like behavior in experimental autoimmune encephalomyelitis, J. Neuroinflammation 13 (2016) 231.
[43] X. Liu, K.P. Connaghan, Y. Wei, Z. Yang, M.D. Li, S.L. Chang, Involvement of the hippocampus in binge ethanol-induced spleen atrophy in adolescent rats, Alcohol. Clin. Exp. Res. 40 (2016) 1489–1500.
[44] H. Offner, S. Subramanian, S.M. Parker, C. Wang, M.E. Afentoulis, A. Lewis, A.A. Vandenbark, P.D. Hurn, Splenic atrophy in experimental stroke is accompanied by increased regulatory T cells and circulating macrophages, J. Immunol. 176 (2006) 6523–6531.
[45] H.A. Seifert, A.A. Hall, C.B. Chapman, L.A. Collier, A.E. Willing, K.R. Pennypacker, A transient decrease in spleen size following stroke corresponds to splenocyte release into systemic circulation, J. NeuroImmune Pharmacol. 7 (2012) 1017–1024.
[46] N. Hara, S. Yoshida, N. Takai, T. Saito, R. Tanaka, Morphological changes of the thymus and spleen with acute experimental allergic encephalomyelitis (EAE) in Lewis rats, No To Shinkei 38 (1986) 81–85.
[47] S. Meyer, M. Strittmatter, C. Fischer, T. Georg, B. Schmitz, Lateralization in autonomic dysfunction in ischemic stroke involving the insular cortex, Neuroreport 15 (2004) 357–361.
[48] C.T. Ajmo, L.A. Collier, C.C. Leonardo, A.A. Hall, S.M. Green, T.A. Womble, J. Cuevas, A.E. Willing, K.R. Pennypacker, Blockade of adrenoreceptors inhibits the splenic response to stroke, Exp. Neurol. 218 (2009) 47–55.
[49] Q. Liu, W.N. Jin, Y. Liu, K. Shi, H. Sun, F. Zhang, C. Zhang, R.J. Gonzales, K.N. Sheth, A. La Cava, F.D. Shi, Brain ischemia suppresses immunity in the periphery and brain via different neurogenic innervations, Immunity 46 (2017) 474–487.
[50] N.L. Chepelev, A.S. Long, A. Williams, B. Kuo, R. Gagne, D.A. Kennedy, D.H. Phillips, V.M. Arlt, P.A. White, C.L.Yauk CL, Transcriptional profiling of dibenzo[def,p]chrysene-induced spleen atrophy provides mechanistic insights into its immunotoxicity in mutamouse, Toxicol. Sci. 149 (2016) 251–268.
[51] J.J. Maher, DAMPs ramp up drug toxicity, J. Clin. Invest. 119 (2009) 246–249.
[52] A.H. Cross, J.L. Stark, JL, Humoral immunity in multiple sclerosis and its animal model, experimental autoimmune encephalomyelitis, Immunol. Res. 32 (2005) 85–97.
[53] H.C. von Büdingen, N. Tanuma, P. Villoslada, J.C. Ouallet, S.L. Hauser, C.P. Genain, Immune responses against the myelin/oligodendrocyte glycoprotein in experimental autoimmune demyelination, J. Clin. Immunol. 21 (2001) 155–170.
[54] K. Lehmann-Horn, S. Kinzel, M.S. Weber, Deciphering the role of B cells in multiple sclerosis-towards specific targeting of pathogenic function, Int. J. Mol. Sci. 18 (2017) 2048 (18 pii: E2048).
[55] K.K. Menon, S.J. Piddlesden, C.C. Bernard, Demyelinating antibodies to myelin oligodendrocyte glycoprotein and galactocerebroside induce degradation of myelin basic protein in isolated human myelin, J. Neurochem. 69 (1997) 214–222.
[56] P. Khare, D.K. Challa, S.C. Devanaboyina, R. Velmurugan, S. Hughes, B.M. Greenberg, R.J. Ober, E.S. Ward, Myelin oligodendrocyte glycoprotein-specific antibodies from multiple sclerosis patients exacerbate disease in a humanized mouse model, J. Autoimmunity 86 (2018) 104–115.
[57] H. Li, M. Zhang, C.C. Wang, X.L. Li, P. Zhang, L.T. Yue, S. Miao, Y.C. Dou, Y.B. Li, R.S. Duan, ROCK inhibitor abolishes the antibody response in experimental autoimmune myasthenia gravis, Mol. Cell. Neurosci. 74 (2016) 106–113.
[58] G. Noorzehi, P. Pasbakhsh, M. Borhani-Haghighi, I.R. Kashani, S. Madadi, F. Tahmasebi, S. Nekoonam, M. Azizi, Microglia polarization by methylprednizolone acetate accelerates cuprizone induced demyelination, J. Mol. Histol. 49 (2018) 471–479.
[59] M.M. Hiremath, Y. Saito, G.W. Knapp, J.P. Ting, K. Suzuki, G.K. Matsushima, Microglial/macrophage accumulation during cuprizone-induced demyelination in C57BL/6 mice, J. Neuroimmunol. 92 (1998) 38–49.
[60] N. Beckmann, E. Giorgetti, A. Neuhaus, S. Zurbruegg, N. Accart, P. Smith, J. Perdoux, L. Perrot, M. Nash, S. Desrayaud, P. Wipfli, W. Frieauff, D.R. Shimshek, Brain region-specific enhancement of remyelination and prevention of demyelination by the CSF1R kinase inhibitor BLZ945, Acta Neuropathol. Commun. 6 (2018) 9, https://doi.org/10.1186/s40478-018-0510-8.
[61] M.W. Salter, B. Stevens, Microglia emerge as central players in brain disease, Nat. Med. 23 (2017) 1018–1027.
[62] A. Van't Veer, Y. Du, T.Z. Fischer, D.R. Boetig, M.R. Wood, C.F. Dreyfus, Brain-derived neurotrophic factor effects on oligodendrocyte progenitors of the basal

forebrain are mediated through trkB and the MAP kinase pathway, J. Neurosci. Res. 87 (2009) 69–78.
[63] M.W. VonDran, H. Singh, J.Z. Honeywell, C.F. Dreyfus, Levels of BDNF impact oligodendrocyte lineage cells following a cuprizone lesion, J. Neurosci. 31 (2011) 14182–14190.
[64] D. Azoulay, V. Vachapova, B. Shihman, A. Miler, A. Karni, Lower brain-derived neurotrophic factor in serum of relapsing remitting MS: reversal by glatiramer acetate, J. Neuroimmunol. 167 (2005) 215–218.
[65] E.R. Frota, D.H. Rodrigues, E.A. Donadi, D.G. Brum, D.R. Maciel, A.L. Teixeira, Increased plasma levels of brain derived neurotrophic factor (BDNF) after multiple sclerosis relapse, Neurosci. Lett. 460 (2009) 130–132.
[66] P. Sarchielli, L. Greco, A. Stipa, A. Floridi, V. Gallai, Brain-derived neurotrophic factor in patients with multiple sclerosis, J. Neuroimmunol. 132 (2002) 180–188.
[67] P. Sarchielli, M. Zaffaroni, A. Floridi, L. Greco, A. Candeliere, A. Mattioni, S. Tenaglia, M. Di Filippo, P. Calabresi, Production of brain-derived neurotrophic factor by mononuclear cells of patients with multiple sclerosis treated with glatiramer acetate, interferon-beta 1a, and high doses of immunoglobulins, Mult. Scler. 13 (2007) 313–331.
[68] M. Caggiula, A.P. Batocchi, G. Frisullo, F. Angelucci, A.K. Patanella, C. Sancricca, V. Nociti, P.A. Tonali, M. Mirabella, Neurotrophic factors in relapsing remitting and secondary progressive multiple sclerosis patients during interferon beta therapy, Clin. Immunol. 118 (2006) 77–82.